

---

# Are Time-Series Foundation Models Deployment-Ready? A Systematic Study of Adversarial Robustness Across Domains

---

**Jiawen Zhang\***  
HKUST (GZ)

Guangzhou, China

jiawe.zh@gmail.com

**Zhenwei Zhang\***  
Tsinghua University

Beijing, China

thuzhangzw@outlook.com

**Shun Zheng†**

Microsoft Research Asia

Beijing, China

shun.zheng@microsoft.com

**Xumeng Wen**

Microsoft Research Asia  
Beijing, China

xumengwen@microsoft.com

**Jia Li†**

HKUST (GZ)  
Guangzhou, China  
jialee@ust.hk

**Jiang Bian**

Microsoft Research Asia  
Beijing, China

jiang.bian@microsoft.com

## Abstract

Time Series Foundation Models (TSFMs), which are pretrained on large-scale, cross-domain data and capable of zero-shot forecasting in new scenarios without further training, are increasingly adopted in real-world applications. However, as the zero-shot forecasting paradigm gets popular, a critical yet overlooked question emerges: Are TSFMs robust to adversarial input perturbations? Such perturbations could be exploited in man-in-the-middle attacks or data poisoning. To address this gap, we conduct a systematic investigation into the adversarial robustness of TSFMs. Our results show that even minimal perturbations can induce significant and controllable changes in forecast behaviors—including trend reversal, temporal drift, and amplitude shift—posing serious risks to TSFM-based services. Through experiments on representative TSFMs and multiple datasets, we reveal their consistent vulnerabilities and identify potential architectural designs, such as structural sparsity and multi-task pretraining, that may improve robustness. Our findings offer actionable guidance for designing more resilient forecasting systems and provide a critical assessment of the adversarial robustness of TSFMs.

## 1 Introduction

Time series forecasting plays a critical role in domains such as finance, energy, transportation, and public health, where accurate predictions are essential for informed decision-making [58, 45, 14, 44]. Inspired by recent advances in vision [33, 3, 51] and language [18, 36, 4, 59], a new generation of Time-Series Foundation Models (TSFMs) [35] has emerged. Pretrained on large-scale, cross-domain data, these models offer strong generalization and zero-shot forecasting capabilities, making them promising candidates for real-world applications, particularly in dynamic or data-scarce environments.

Yet, before TSFMs can be safely deployed, a fundamental question remains: *Are these models robust to adversarial input perturbations?* Unlike images or text, time-series inputs exhibit strong temporal dependencies and lack semantic interpretability, making them especially susceptible to subtle manipulations. Malicious actors could exploit these properties to launch man-in-the-middle attacks or

---

\*This work was done while the author was an intern at Microsoft Research Asia.

†Corresponding Author.

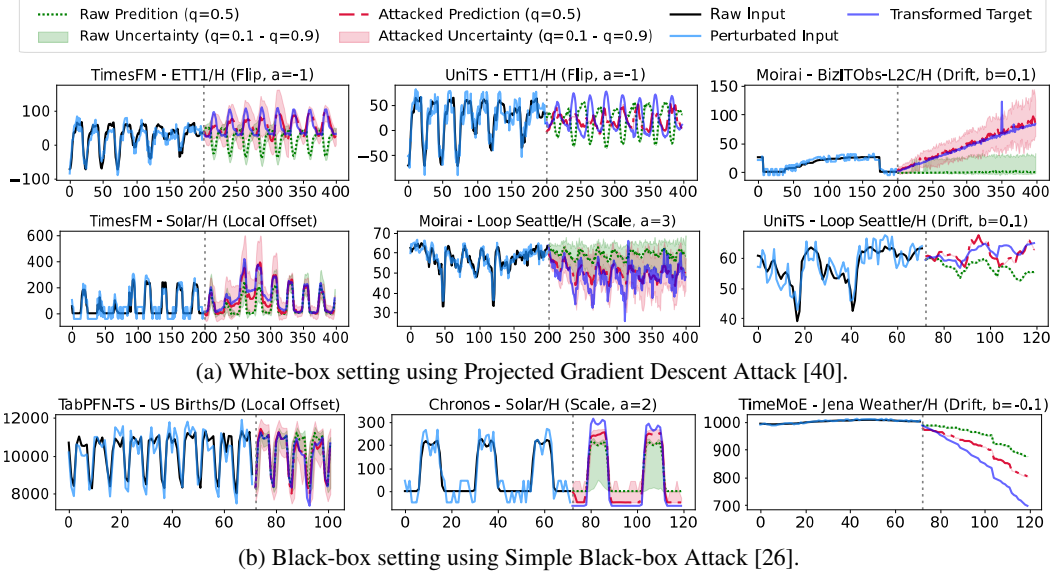


Figure 1: **Visualization of targeted adversarial attacks on TSFMs across diverse domains.** This figure illustrates how **adversarial perturbations** guide model forecasts toward specific target behaviors (i.e., **transformed target**) including pattern flipping, local offsets, scaling, and long-term drifts. We evaluate six representative TSFMs (TimesFM, UniTS, Moirai, TabPFN-TS, Chronos, and TimeMoE) across datasets from energy, weather, transportation, web, healthcare, and sales.

data poisoning, thereby steering forecasts toward harmful outcomes such as trend reversals, amplitude shifts, or delayed reactions. In high-stakes settings, even small perturbs can lead to cascading failures, e.g., financial manipulation, infrastructure misallocation, or public service disruption.

While adversarial robustness has been extensively studied in computer vision [57, 24, 28, 9, 40, 8, 26, 43] and language models [53, 27, 16, 60, 61, 34], its implications for TSFMs remain largely underexplored. Given the growing attention on zero-shot forecasting and the increasing ambition to unify models across domains, evaluating the security and reliability of TSFMs under adversarial conditions is both timely and essential.

To fill this gap, we conduct a systematic study on the adversarial robustness of time-series foundation models under different threat models. As illustrated in Figure 1, we show that even minimal, well-crafted perturbations can reliably steer model forecasts toward specific target behaviors, such as flipping trends, inducing drifts, or shifting amplitudes, without requiring access to future ground-truth labels. Our analysis further identifies architectural features, such as structural sparsity and multi-task pretraining, that contribute to enhanced robustness against such adversarial attacks.

**Main Contributions.** We propose a unified adversarial assessment protocol for TSFMs (Figure 2) that covers a wide spectrum of threat models by varying the adversary’s *objective* (untargeted vs. targeted), *capability* (perturbation constraints), and *knowledge* (white-box vs. black-box). Using this framework, we evaluate six representative TSFMs across diverse forecasting domains and input distributions. Our experiments uncover consistent vulnerabilities across models and attack settings. We further analyze how factors such as perturbation budget, input context length, model scale, and attack location influence adversarial effectiveness. Together, our findings offer a quantitative understanding of TSFMs’ adversarial susceptibility and deliver actionable insights for developing more resilient and deployment-ready forecasting systems.

## 2 Related Work

**Foundation Models for Time Series Forecasting.** Inspired by the success of foundation models in language [4], a growing number of time-series foundation models have emerged [13, 49, 2, 54, 62, 19, 29, 25, 22, 39, 12, 63, 66, 6, 23, 5, 47]. Despite differences in backbone architecture,

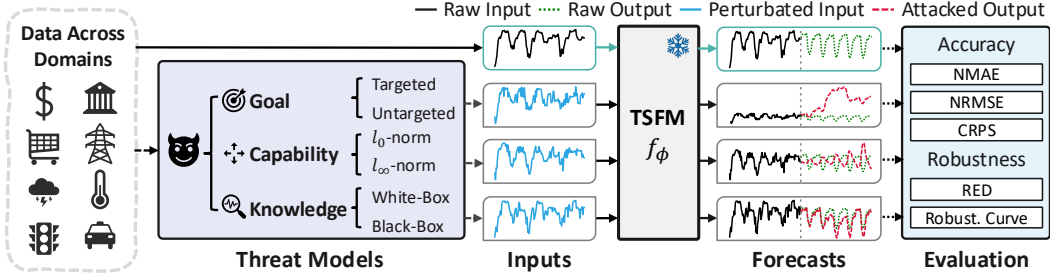


Figure 2: **Overview of the adversarial evaluation protocol for time-series foundation models.** We evaluate TSFMs across diverse domains under a unified adversarial framework. The threat model is defined by three key dimensions: adversary *goal*, *capability*, and *knowledge*. Adversarial perturbations are applied to raw inputs, which are then passed through the TSFM to produce perturbed forecasts. We assess the impact of these attacks by comparing raw and attacked outputs using both accuracy metrics and robustness indicators.

optimization objectives, and data regimes, these TSFMs share a common objective: achieving universal forecasting capability. However, this pursuit of universality and accuracy has often come at the expense of robustness [30, 56]. As TSFMs move closer to real-world deployment, their susceptibility to input perturbations and adversarial threats raises important concerns about their reliability. In this work, we conduct a systematic adversarial robustness evaluation across six representative TSFMs: TimesFM [13], TimeMoE [54], UniTS [22], Moirai [62], Chronos [2], and TabPFN-TS [29]. A detailed comparison of model characteristics is provided in Appendix A.

**Adversarial Robustness in Deep Neural Networks.** Adversarial robustness has become a critical focus in deep learning, especially for safety-sensitive applications. It is well established that deep neural networks are highly vulnerable to imperceptible input perturbations that can lead to significant prediction errors [57, 24]. This discovery sparked a wave of research on robustness evaluation, resulting in the development of standardized benchmarking frameworks and attack methods in computer vision [7, 38, 21, 17, 10]. With the rapid advancement and widespread adoption of large language models and vision-language foundation models, adversarial robustness in these systems has also attracted growing attention [53, 27, 46, 67, 52].

In contrast, adversarial robustness in time series models, particularly for forecasting, remains underexplored. Prior work has largely focused on classification tasks [55, 50, 31, 20, 15], or on constructing adversarial examples for specific forecasting architectures [11, 64, 37]. While these studies demonstrate that time series models are indeed susceptible to adversarial perturbations, they primarily address small-scale models or narrow domain settings. The robustness of large-scale, pretrained TSFMs has yet to be systematically investigated, and their behavior under adversarial conditions remains largely unknown. In this study, we present the first comprehensive and quantitative assessment of adversarial vulnerability in TSFMs. Our goal is to bring attention to the robustness challenges in time series forecasting and establish a foundation for future work in this critical but overlooked area.

### 3 Adversarial Evaluation Protocol

We introduce an evaluation protocol designed to assess the adversarial robustness of time-series foundation models under realistic threat models. As illustrated in Figure 2, the protocol consists of three core components: threat model specification (Section 3.2), construction of adversarial perturbations (Section 3.3), and evaluation of in terms of accuracy and robustness (Section 3.4).

#### 3.1 Preliminaries

**Time-Series Forecasting.** We consider a univariate time series  $\mathbf{x}_{1:T} = \{x_\tau\}_{\tau=1}^T$ , where each observation  $x_\tau \in \mathbb{R}$  corresponds to the value at time step  $\tau$ . A forecasting model  $f_\phi$  with parameters  $\phi$  maps an input sequence of length  $L$  to a prediction over the future  $T$  steps  $f_\phi : \mathbf{x}_{t-L:t} \mapsto \hat{\mathbf{x}}_{t+1:t+T}$ , where  $\hat{\mathbf{x}}_{t+1:t+T}$  is the predicted future trajectory. The model is typically trained by minimizing the expected forecasting loss:  $\min_\phi \mathbb{E}_{\mathbf{x} \sim \mathcal{P}(\mathcal{D}), t \sim \mathcal{P}(\mathcal{T})} [\mathcal{L}(f_\phi(\mathbf{x}_{t-L:t}), \mathbf{x}_{t+1:t+T})]$ , where  $\mathcal{P}(\mathcal{D})$  is

Table 1: Parameter settings for different target transformations used in targeted adversarial attacks. Each transformation modifies the forecast in a specific pattern by configuring the scaling factor  $a$  and time-dependent bias  $c(\tau)$ . Here,  $b \in \mathbb{R}$  controls the drift strength,  $\delta_\tau \in \mathbb{R}$  specifies localized shifts, and  $\mathcal{I} \subseteq \{1, \dots, T\}$  denotes the perturbed forecast steps. See Figure 3 for transformation examples.

Transformation	Parameters	Description
Scaling	$a > 0, c(\tau) = 0$	Uniformly scales the forecast
Flipping	$a < 0, c(\tau) = 0$	Reflects the sequence
Drifting	$a = 1, c(\tau) = b \cdot \tau$	Adds global linear drift
Local Offsetting	$a = 1, c(\tau) = \delta_\tau$ if $\tau \in \mathcal{I}$	Perturbs selected steps only

the data distribution,  $\mathcal{P}(\mathcal{T})$  is the sampling distribution over timestamps, and  $\mathcal{L}$  is the loss function. TSFMs are typically pretrained on large-scale, multi-domain datasets, and their parameters  $\phi$  remain frozen during downstream deployment. To better reflect real-world conditions, we conduct adversarial evaluation at inference time by perturbing the input to generate adversarial examples.

**Threat Model.** An *Adversarial sample* is constructed by adding a small perturbation  $\delta \in \mathbb{R}^L$  such that the perturbed input  $\mathbf{x}^{\text{adv}} = \mathbf{x} + \delta$  causes the model’s output to deviate significantly from its prediction on the original input  $\mathbf{x}$ . The *threat model* characterizes the assumptions made about the adversary in terms of their goals, capabilities, and knowledge [7]. The adversary’s goal determines the intended effect of the attack on the model’s output, either to degrade performance without a specific target (untargeted), or to manipulate the output toward a predefined outcome (targeted). Their capability refers to the extent of input perturbations they are allowed to make, typically bounded by an  $\ell_p$ -norm constraint  $|\delta|_p \leq \epsilon$ , where  $\epsilon$  controls the perturbation budget and  $p$  (commonly 0, 2, or  $\infty$ ) defines the perturbation geometry. Finally, the adversary’s knowledge reflects the information they possess about the model. In a white-box setting, the attacker has full access to the model architecture and parameters, while in a black-box setting, access is limited to input-output queries without internal details, e.g., only able to obtain the prediction from API.

### 3.2 Threat Model Specification for TSFMs

**Attack Objective.** We formulate adversarial example construction for time-series forecasting as a unified optimization problem. Given an input sequence  $\mathbf{x}_{t-L:t} \in \mathbb{R}^L$ , a pre-trained forecasting model  $f_\phi$ , and a reference sequence  $\mathbf{y} \in \mathbb{R}^T$  (which may represent the ground-truth, raw prediction, or an attacker-defined target), the goal is to find a perturbation  $\delta \in \mathcal{S} \subseteq \mathbb{R}^L$  such that the model’s output on the perturbed input significantly deviates from—or closely matches—the reference. Specifically, we define the general attack objective as:

$$\delta^* = \arg \max_{\delta \in \mathcal{S}} [\sigma \cdot \mathcal{L}(f_\phi(\mathbf{x}_{t-L:t} + \delta), \mathbf{y})], \quad (1)$$

where  $\mathcal{L}(\cdot, \cdot)$  is a forecasting loss function (e.g., MSE, MAE), and  $\sigma \in \{+1, -1\}$  indicates the attack direction:  $\sigma = +1$  for *untargeted attacks* (maximizing prediction error with respect to the raw output), and  $\sigma = -1$  for *targeted attacks* (minimizing error toward a predefined target  $\mathbf{y}$ ). The perturbation set  $\mathcal{S} \subseteq \mathbb{R}^L$  specifies the allowable perturbations. For clarity, we denote the overall attack objective as:

$$g_\phi(\delta) := \sigma \cdot \mathcal{L}(f_\phi(\mathbf{x}_{t-L:t} + \delta), \mathbf{y}), \quad (2)$$

which unifies both attack types under a single formulation. Due to the unavailability of ground-truth future values at inference time, we treat the model’s raw prediction as the attack target  $\mathbf{y}$ .

**Building Targets for Targeted Attacks.** To evaluate the performance of TSFMs under targeted attacks, we first construct appropriate target trajectories. Intuitively, adversarial targets should remain related to the model’s original predictions, rather than being entirely uncorrelated. In practice, attackers often seek to introduce subtle but systematic deviations—such as periodic shifts or gradual drifts—that are difficult to detect yet can accumulate significant downstream effects. To support controlled experimentation, the extent of deviation from the raw forecast should be adjustable, enabling us to examine how susceptible the model is to both mild and aggressive manipulations.

To this end, we define a family of transformation functions  $\mathcal{M}(\cdot)$  that generate adversarial targets by applying structured modifications to the raw forecast. Given a raw prediction  $\hat{\mathbf{x}} = \{\hat{x}_\tau\}_{\tau=1}^T$ , the

transformed target sequence  $\mathbf{y} = \{y_\tau\}_{\tau=1}^T$  is computed as:

$$y_\tau = \mathcal{M}(\hat{x}_\tau; a, c) = a \cdot \hat{x}_\tau + c(\tau), \quad (3)$$

where  $a \in \mathbb{R}$  controls the amplitude (scaling), and  $c(\tau)$  is a time-dependent bias function. By tuning  $a$  and the shape of  $c(\tau)$ , we instantiate various adversarial patterns with adjustable distortion levels.

Table 1 summarizes the transformation types considered in our evaluation, and Figure 1 and 3 illustrates visual examples of the resulting targets. While we focus on representative manipulation patterns in this study, the proposed formulation can be readily extended to broader classes of adversarial objectives.

**Perturbation Budget.** The perturbation budget directly reflects the strength of the attack. Larger perturbations tend to cause greater deviations in model outputs, but excessive distortion may lead to unrealistic inputs that compromise both the fairness of robustness evaluation and the plausibility of real-world scenarios. For time-series data, two factors are particularly important: the number of perturbed time steps, and the magnitude of each perturbation. As a result, a single  $\ell_p$ -norm constraint is insufficient and finer-grained control is required.

Motivated by this, we impose a *hybrid norm constraint* that jointly bounds perturbation sparsity and amplitude. The feasible perturbation set is defined as:

$$\mathcal{S} = \{\boldsymbol{\delta} \in \mathbb{R}^L : \|\boldsymbol{\delta}\|_0 \leq rL, \|\boldsymbol{\delta}\|_\infty \leq \epsilon\}, \quad (4)$$

where  $r \in (0, 1]$  denotes the *perturbation ratio* (the fraction of time steps modified), and  $\epsilon > 0$  is the *per-element perturbation bound* (the maximum change per step).

When  $r < 1$ , the attacker must select a subset of time steps to perturb. However, exhaustively identifying the most impactful positions is computationally expensive, particularly for long input sequences. Based on our empirical finding that time steps closer to the forecast horizon tend to be more vulnerable (see Section 4.2), we default to perturbing the final  $rL$  time steps unless otherwise stated. Besides, to ensure consistency across time series of different scales, we normalize the perturbation bound adaptively using the input variance:  $\epsilon^* = \epsilon \cdot \text{var}(\mathbf{x})$ , where  $\text{var}(\mathbf{x})$  denotes the variance of the input sequence.

### 3.3 Adversarial Perturbation Optimization

Since TSFMs differ in model accessibility, we select appropriate adversarial optimization strategies based on the adversary’s level of knowledge for evaluation.

**White-Box Attack Setting.** In the white-box setting, the attacker has full access to the model architecture, parameters  $\phi$ . We employ *Projected Gradient Descent (PGD)* [40], a widely used and reliable method that serves as the foundation for many subsequent attack methods. PGD iteratively updates the perturbation via:

$$\boldsymbol{\delta}^{k+1} = \Pi_{\mathcal{S}}(\boldsymbol{\delta}^k + \alpha \cdot \text{sgn}(\nabla_{\boldsymbol{\delta}} g_{\phi}(\boldsymbol{\delta}^k))), \quad (5)$$

where  $\alpha$  is the step size,  $\Pi_{\mathcal{S}}$  denotes projection onto the feasible set  $\mathcal{S}$ , and  $k$  is the iteration index.

**Black-Box Attack Setting.** In the black-box setting, the attacker has no access to model internals and must rely solely on input-output queries to estimate effective perturbations. We implement two representative black-box attacks: *Zero-Order Optimization*[8] and *Simple Black-box Attack*[26].

*Zero-Order Optimization (ZOO)* estimates gradients using finite differences. For the  $i$ -th component, the directional derivative is approximated as:

$$\nabla_i g_{\phi}(\boldsymbol{\delta}) \approx \frac{g_{\phi}(\boldsymbol{\delta} + \mu \mathbf{u}_i) - g_{\phi}(\boldsymbol{\delta})}{2\mu}, \quad (6)$$

where  $\mathbf{u}_i$  is the  $i$ -th standard basis vector and  $\mu > 0$  is a small constant. The estimated gradients are then used to update  $\boldsymbol{\delta}$  as PGD did. We also implement a *ZOO-Adam* variant that applies the Adam optimizer to the estimated gradients to improve stability and convergence.

*Simple Black-box Attack (SimBA)* performs a query-efficient random search over a predefined orthogonal basis. At each iteration, a direction  $\mathbf{q} \in Q$  is sampled without replacement, and the perturbation is updated based on whether it improves the attack objective:

$$\delta^{k+1} = \begin{cases} \delta^k + \alpha\mathbf{q}, & \text{if } g_\phi(\delta^k + \alpha\mathbf{q}) > g_\phi(\delta^k), \\ \delta^k - \alpha\mathbf{q}, & \text{if } g_\phi(\delta^k - \alpha\mathbf{q}) > g_\phi(\delta^k), \\ \delta^k, & \text{otherwise.} \end{cases} \quad (7)$$

To better align SimBA with the characteristics of time-series data, we explore three orthogonal basis designs: Cartesian (point-wise), DCT (low-frequency), and Wavelet (time-frequency). These bases enable perturbations with distinct structural properties. Full definitions and implementation details are provided in Appendix B.1.

### 3.4 Evaluation Metrics and Protocols

**Forecasting Accuracy.** To measure accuracy, we compute the discrepancy between the model’s predictions and ground truth before and after perturbation. We adopt three widely used metrics: *Normalized Mean Absolute Error (NMAE)*, *Normalized Root Mean Squared Error (NRMSE)*, and *Continuous Ranked Probability Score (CRPS)*. Details of all metrics are provided in Appendix B.2.

**Adversarial Robustness.** Robustness is quantified by measuring how forecasting performance changes under adversarial perturbations. This evaluation poses two challenges: (i) Since ground truth is unavailable during attack construction, we use the model’s raw prediction as a surrogate target. However, this introduces a bias, as robustness scores are no longer directly comparable across models with different baseline errors. (ii) The opposing goals of targeted and untargeted attacks, i.e., minimizing vs. maximizing forecast error, require a unified metric to enable consistent evaluation.

We introduce the *Relative Error Deviation (RED <sub>$\mathcal{E}$</sub> )* to address both challenges. It captures the relative change in forecasting error in a direction-consistent manner. Let  $\mathcal{E}(\cdot, \cdot)$  denote a forecasting error metric (e.g., NMAE), and let  $\hat{\mathbf{x}}^{\text{raw}}$ ,  $\hat{\mathbf{x}}^{\text{adv}}$ , and  $\mathbf{y}$  be the raw prediction, adversarial prediction, and reference sequence, respectively. We define RED <sub>$\mathcal{E}$</sub>  as:

$$\text{RED}_{\mathcal{E}} = \frac{\mathcal{E}_{\text{attack}}}{\mathcal{E}^{\text{raw}} + \varepsilon}, \quad \mathcal{E}_{\text{attack}} = \begin{cases} \mathcal{E}^{\text{adv}} - \mathcal{E}^{\text{raw}}, & \text{untargeted attack,} \\ \mathcal{E}^{\text{raw}} - \mathcal{E}^{\text{adv}}, & \text{targeted attack,} \end{cases} \quad (8)$$

where  $\mathcal{E}^{\text{raw}} = \mathcal{E}(\hat{\mathbf{x}}^{\text{raw}}, \mathbf{y})$  and  $\mathcal{E}^{\text{adv}} = \mathcal{E}(\hat{\mathbf{x}}^{\text{adv}}, \mathbf{y})$ , and  $\varepsilon > 0$  is a small constant. RED <sub>$\mathcal{E}$</sub>  reflects the relative degradation or improvement in model predictions compared to the raw baseline. Higher values indicate more effective attacks, whether by increasing error in untargeted settings or reducing it toward a desired target in targeted scenarios. RED <sub>$\mathcal{E}$</sub>  = 0 means the attack has no effect, and the model performs identically to its clean prediction.

While RED <sub>$\mathcal{E}$</sub>  offers a unified view, it may overestimate attack effectiveness when a model’s raw error is very low, leading to a large RED despite acceptable post-attack performance. To complement this, we also plot *robustness curves*, which visualize the absolute forecasting error under varying perturbation budgets, providing a more comprehensive robustness profile. The complete evaluation procedure is summarized in Algorithm 1.

## 4 Results and Analyses

In this section, we demonstrate the adversarial robustness of representative time series foundation models. Section 4.1 provides an overall assessment of model robustness and attack effectiveness, and Section 4.2 further investigates how key factors, including perturbation budget, attack position, context length, and model size, affect the adversarial impacts. We leave more details of experiments and results in Appendix C and D.

**Datasets.** We evaluate model robustness on eight datasets from the GIFT-Eval benchmark [1], spanning diverse domains and sampling frequencies. Unless otherwise specified, all experiments are conducted in the short-term forecasting setting. Results under medium- and long-term prediction horizons are provided in Appendix D.7 for completeness. For short-term forecasting, we use a fixed input context length of 128 across all datasets. Additional dataset details, including domain characteristics and prediction lengths, are summarized in Table 4.

Table 2: **Untargeted attacks against TSFMs.** We report the  $\text{RED}_{\text{NMAE}}$  averaged across attack budgets ( $\epsilon \in \{0.25, 0.5, 0.75, 1\}$ ,  $r \in \{0.25, 0.5, 0.75, 1\}$ ) and datasets. **Red** is used to denote the model most impacted by the attack. Clean forecasting performance is provided in Table 5.

Dataset	PGD				SimBA					
	TimesFM	TimeMoE	UniTS	Moirai	TimesFM	TimeMoE	UniTS	Moirai	Chronos	TabPFN-TS
Loop Seattle	27.45	0.25	0.34	1.61	0.96	0.39	0.01	0.44	0.15	0.84
BizITObs-L2C	14.59	0.22	0.43	0.35	1.47	0.47	0.13	0.39	0.20	0.52
Electricity	27.25	0.19	0.18	0.31	1.45	0.37	0.00	0.06	0.05	0.53
ETT1	32.45	0.20	0.58	1.63	1.66	0.80	0.06	0.63	0.50	1.36
Hier. Sales	45.28	0.08	1.46	1.16	3.99	0.71	0.23	0.40	0.58	2.17
Jena Weather	38.32	0.04	0.40	0.64	2.19	0.41	0.04	0.13	0.19	1.25
Solar	48.79	0.65	0.34	1.05	3.03	1.43	0.06	0.72	0.63	1.64
US Births	30.28	0.81	0.06	0.59	3.16	1.60	-0.01	0.39	1.11	2.50

**Time-series Foundation Models.** We select six representative models for evaluation, including TimesFM (200M) [13], TimeMoE (base) [54], UniTS (x128) [22], Moirai (base) [62], Chronos (small) [2], and TabPFN-TS [29]<sup>3</sup>. These models differ in terms of architecture, decoding strategy, prediction head (point vs. probabilistic forecasting), and training paradigms. This diversity allows us to investigate how different design choices impact adversarial robustness. A detailed comparison of the models is provided in Table 3.

**Evaluation Setup.** All models are evaluated using their official released checkpoints with parameters kept frozen. PGD and ZOO attacks use a step size of  $\alpha = 0.05$ , with PGD running for 300 iterations and ZOO limited to 500 queries. SimBA’s iteration count varies based on the basis dimensionality and attack budget due to its sampling scheme. Experiments are run on a single NVIDIA Tesla V100 GPU with CUDA 12.1. We report NMAE and  $\text{RED}_{\text{NMAE}}$  as primary metrics for forecasting accuracy and robustness, respectively. See Appendix B.2 for more details.

#### 4.1 Adversarial Robustness of TSFMs

**Subtle perturbations can cause severe degradation in forecast accuracy.** Our results show that most TSFMs are highly susceptible to adversarial attacks, with varying degrees of vulnerability across models. As shown in Table 2, TimesFM and TabPFN-TS exhibit particularly high sensitivity. Surprisingly, PGD attacks on TimesFM result in forecast errors up to 50 times higher than clean performance. For TabPFN-TS, the backbone was not originally trained for time series forecasting, potentially leading to poor generalization under perturbed conditions. Other models also exhibit significant degradation, highlighting adversarial vulnerability as a common concern in current TSFMs.

**Targeted behaviors can be induced even under small perturbation budgets.** As illustrated in Figure 1 and 3, targeted attacks can successfully manipulate TSFM outputs to match specific trajectories, even under small perturbation budgets. Interestingly, we find that attacks targeting the overall shape or trend of the forecast (e.g., scaling or shifting) are consistently more effective than those modifying only a local segment (e.g., local offset), as indicated by the higher RED scores in Tables 7 and 8. This suggests that TSFMs may lack strong global consistency constraints, making them easier to guide toward holistic patterns. In contrast, localized perturbations are often less effective, likely due to the model’s reliance on contextual smoothing and local temporal dependencies. These internal dynamics make it difficult to isolate and alter a specific region without disrupting the broader sequence coherence. A robust model should resist both types of manipulations, particularly when perturbations are minimal, by preserving the structure of the predicted sequence.

**Certain architectural design and training paradigms may offer implicit robustness.** TimeMoE resists gradient-based attacks like PGD, likely due to its MoE gating mechanism disrupting gradient flow—consistent with prior findings on MoE robustness [48]. However, it remains vulnerable to black-box attacks. UniTS demonstrates relative strong robustness against both white-box and black-box attacks. We attribute this to its multi-task pretraining strategy, which has been shown to improve model generalization and stability under adversarial conditions [41].

<sup>3</sup>Unless otherwise specified, we use the model size indicated in parentheses.

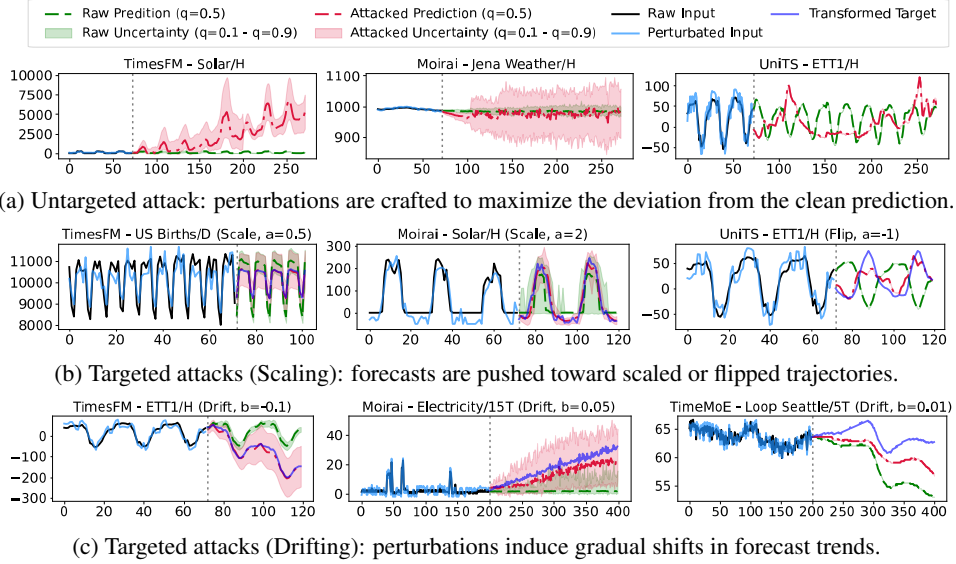


Figure 3: **Visualization of untargeted and targeted adversarial attacks on TSFMs.** In both settings, perturbations are applied with a budget of  $\epsilon \in [0.25, 5]$  and attack ratio  $r \in [0.5, 1]$ . RED<sub>NMAE</sub> scores for various target transformations are provided in Appendix Tables 7 and 8.

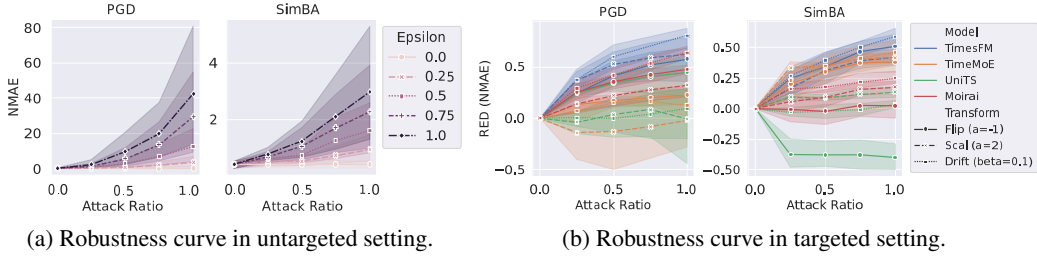


Figure 4: **Impact of perturbation budgets.** (a) For untargeted attacks, we report NMAE across varying attack budgets (i.e.,  $r$  and  $\epsilon$ ). (b) For targeted attacks, we use RED<sub>NMAE</sub> to measure alignment between the perturbed prediction and the target, where higher values indicate more successful attacks.

## 4.2 Further Analyses

**Gradient-based attacks are strong, but not always sufficient.** PGD generally outperforms black-box methods, while SimBA is moderately effective and ZOO is weakest (Appendix D.3). However, their effectiveness is not universal. Models like Chronos and TabPFN-TS apply input discretization, limiting gradient accessibility, while TimeMoE’s gating mechanism in its mixture-of-experts architecture may disrupt gradient flow, weakening the impact of gradient-based attacks. In addition, the choice of perturbation basis influences attack strength. Figure 7b shows that the wavelet-based perturbations outperform DCT and point-wise strategies. These results highlight the need to align attack strategies with model architecture and data properties.

**Adversarial impact increases with attack budget, while targeted attacks exhibit saturation.** As shown in Figure 4, increasing the perturbation budget ( $\epsilon$  or attack ratio  $r$ ) leads to stronger degradation under untargeted and closer to targets in targeted settings. For untargeted attacks, especially under white-box conditions, high budgets result in substantial performance drops. For targeted attacks, however, we observe saturation: once the perturbation budget surpasses a certain threshold, further increases do not improve alignment with the target and may even reduce it due to oversteering.

**Points near the forecast boundary are most vulnerable.** We analyze input sensitivity by computing gradient magnitudes with respect to the attack objective and identifying the top-k most vulnerable

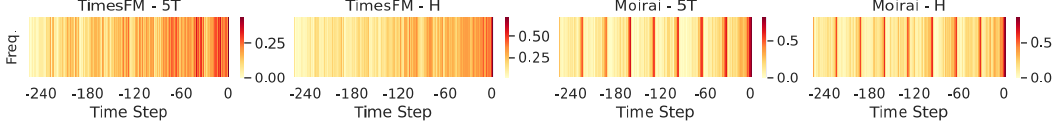


Figure 5: **Impact of perturbation locations.** Darker colors indicate higher frequencies at which a time point is identified as one of the most vulnerable. For each input time step, we compute the gradient magnitude wrt. the attack objective and select the top-25 positions with the highest values as the most sensitive points. We aggregate statistics across datasets with different sampling frequencies.

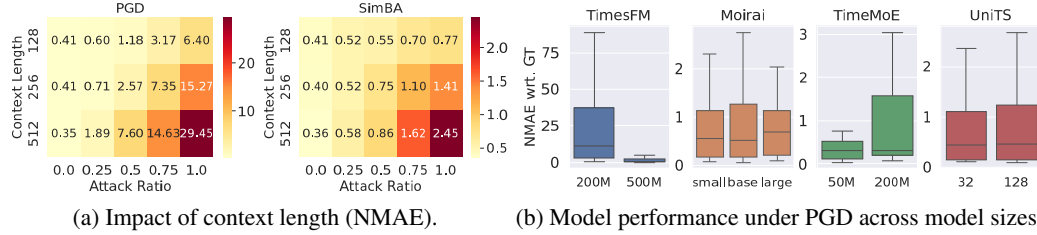


Figure 6: **Effects of context length and model size on adversarial robustness.** (a) NMAE under varying context lengths and attack ratios with PGD and SimBA attacks ( $\epsilon = 0.5$ ). Higher values indicate greater performance degradation. (b) Comparison of model vulnerability under PGD attacks ( $\epsilon = 0.5, r = 1$ ) across different model sizes. Results under SimBA are provided in Appendix D.6.

input positions (Figure 5). A clear pattern emerges: points closer to the forecast horizon consistently exhibit higher vulnerability. Additionally, vulnerability appears model-specific. For instance, Moirai shows consistent sensitivity at specific time positions across datasets, potentially due to its patch-based input configuration.

**Longer contexts enhance clean accuracy but amplify attack effects.** Table 6a shows a trade-off: longer input contexts boost clean accuracy but also enlarge the attack surface. Under PGD with  $r = 0.5$ , extending the context from 128 to 512 increases forecasting error by over 7 $\times$ . This is especially concerning for models like Moirai, which depend on long contexts, highlighting the need to balance accuracy and adversarial robustness.

**Larger models tend to be more vulnerable to gradient-based attacks.** As shown in Table 6b, we observe a clear trend: models with larger parameter counts are generally more susceptible to gradient-based attacks. This may be due to the expanded capacity increasing the number of exploitable directions in the input space. An exception is TimesFM, where the 200M variant is more vulnerable than the 500M version. On the other hand, under black-box attacks (Appendix Table 9), model size does not show a consistent effect on robustness. These findings suggest that while scaling up model size can improve forecasting performance, it may also amplify vulnerability.

## 5 Discussion

This work presents the first systematic study of adversarial robustness in time-series foundation models. We show that small, crafted perturbations can severely degrade performance or induce targeted outputs. To enable rigorous evaluation, we propose a unified protocol covering diverse threat models, attack strategies, and robustness metrics. Our findings reveal widespread vulnerabilities, underscoring the need for more robust TSFMs.

**Broader Impacts.** While our goal is to uncover and understand TSFM vulnerabilities, the techniques developed in this study could be misused. We therefore emphasize the importance of responsible use and advocate for parallel research into effective defense strategies.

**Limitations and Future Work.** Our evaluation focuses on a set of standard attack methods—sufficient for comparative analysis, but not exhaustive. Moreover, our primary goal is diagnostic: to reveal model weaknesses rather than to mitigate them. Future work should explore

defenses tailored to time-series forecasting, including adversarial training, detection mechanisms, and certified robustness. A key challenge remains in balancing robustness with forecasting accuracy to ensure TSFMs are both safe and effective in real-world deployment.

## References

- [1] Taha Aksu, Gerald Woo, Juncheng Liu, Xu Liu, Chenghao Liu, Silvio Savarese, Caiming Xiong, and Doyen Sahoo. 2024. GIFT-Eval: A Benchmark For General Time Series Forecasting Model Evaluation. *arXiv preprint arXiv:2410.10393* (2024).
- [2] Abdul Fatir Ansari, Lorenzo Stella, Caner Turkmen, Xiyuan Zhang, Pedro Mercado, Huibin Shen, Oleksandr Shchur, Syama Sundar Rangapuram, Sebastian Pineda Arango, Shubham Kapoor, et al. 2024. Chronos: Learning the language of time series. *arXiv preprint arXiv:2403.07815* (2024).
- [3] Tim Brooks, Bill Peebles, Connor Holmes, Will DePue, Yufei Guo, Li Jing, David Schnurr, Joe Taylor, Troy Luhman, Eric Luhman, Clarence Ng, Ricky Wang, and Aditya Ramesh. 2024. Video generation models as world simulators. (2024). <https://openai.com/research/video-generation-models-as-world-simulators>
- [4] Tom Brown, Benjamin Mann, Nick Ryder, Melanie Subbiah, Jared D Kaplan, Prafulla Dhariwal, Arvind Neelakantan, Pranav Shyam, Girish Sastry, Amanda Askell, et al. 2020. Language models are few-shot learners. In *NeurIPS*. 1877–1901.
- [5] Defu Cao, Furong Jia, Sercan O Arik, Tomas Pfister, Yixiang Zheng, Wen Ye, and Yan Liu. 2024. Tempo: Prompt-based generative pre-trained transformer for time series forecasting. In *CILR*.
- [6] Defu Cao, Wen Ye, Yizhou Zhang, and Yan Liu. 2024. Timedit: General-purpose diffusion transformers for time series foundation model. *arXiv preprint arXiv:2409.02322* (2024).
- [7] Nicholas Carlini, Anish Athalye, Nicolas Papernot, Wieland Brendel, Jonas Rauber, Dimitris Tsipras, Ian Goodfellow, Aleksander Madry, and Alexey Kurakin. 2019. On evaluating adversarial robustness. *arXiv preprint arXiv:1902.06705* (2019).
- [8] Pin-Yu Chen, Huan Zhang, Yash Sharma, Jinfeng Yi, and Cho-Jui Hsieh. 2017. Zoo: Zeroth order optimization based black-box attacks to deep neural networks without training substitute models. In *Proceedings of the 10th ACM workshop on artificial intelligence and security*. 15–26.
- [9] Joana C Costa, Tiago Roxo, Hugo Proen  a, and Pedro Ricardo Morais Inacio. 2024. How deep learning sees the world: A survey on adversarial attacks & defenses. *IEEE Access* 12 (2024), 61113–61136.
- [10] Francesco Croce, Maksym Andriushchenko, Vikash Sehwag, Edoardo Debenedetti, Nicolas Flammarion, Mung Chiang, Prateek Mittal, and Matthias Hein. 2021. Robustbench: a standardized adversarial robustness benchmark. In *NeurIPS*.
- [11] Rapha  l Dang-Nhu, Gagandeep Singh, Pavol Bielik, and Martin Vechev. 2020. Adversarial attacks on probabilistic autoregressive forecasting models. In *ICML*. 2356–2365.
- [12] Luke Nicholas Darlow, Qiwen Deng, Ahmed Hassan, Martin Asenov, Rajkarn Singh, Artjom Joosen, Adam Barker, and Amos Storkey. 2024. DAM: Towards a Foundation Model for Forecasting. In *ICLR*.
- [13] Abhimanyu Das, Weihao Kong, Rajat Sen, and Yichen Zhou. 2024. A decoder-only foundation model for time-series forecasting. In *ICML*.
- [14] Franca Rocco di Torrepadula, Enea Vincenzo Napolitano, Sergio Di Martino, and Nicola Mazzocca. 2024. Machine Learning for public transportation demand prediction: A Systematic Literature Review. *Engineering Applications of Artificial Intelligence* 137 (2024), 109166.
- [15] Daizong Ding, Mi Zhang, Fuli Feng, Yuanmin Huang, Erling Jiang, and Min Yang. 2023. Black-box adversarial attack on time series classification. In *AAAI*, Vol. 37. 7358–7368.

[16] Xinshuai Dong, Anh Tuan Luu, Min Lin, Shuicheng Yan, and Hanwang Zhang. 2021. How should pre-trained language models be fine-tuned towards adversarial robustness?. In *NeurIPS*. 4356–4369.

[17] Yinpeng Dong, Qi-An Fu, Xiao Yang, Tianyu Pang, Hang Su, Zihao Xiao, and Jun Zhu. 2020. Benchmarking adversarial robustness on image classification. In *CVPR*. 321–331.

[18] Abhimanyu Dubey, Abhinav Jauhri, Abhinav Pandey, Abhishek Kadian, Ahmad Al-Dahle, Aiesha Letman, Akhil Mathur, Alan Schelten, Amy Yang, Angela Fan, et al. 2024. The llama 3 herd of models. *arXiv preprint arXiv:2407.21783* (2024).

[19] Vijay Ekambaram, Arindam Jati, Nam H Nguyen, Pankaj Dayama, Chandra Reddy, Wesley M Gifford, and Jayant Kalagnanam. 2024. Tiny Time Mixers (TTMs): Fast Pre-trained Models for Enhanced Zero/Few-Shot Forecasting of Multivariate Time Series. *arXiv preprint arXiv:2401.03955* (2024).

[20] Hassan Ismail Fawaz, Germain Forestier, Jonathan Weber, Lhassane Idoumghar, and Pierre-Alain Muller. 2019. Adversarial attacks on deep neural networks for time series classification. In *IJCNN*. 1–8.

[21] Ruize Gao, Jiongxiao Wang, Kaiwen Zhou, Feng Liu, Binghui Xie, Gang Niu, Bo Han, and James Cheng. 2022. Fast and reliable evaluation of adversarial robustness with minimum-margin attack. In *ICML*. PMLR, 7144–7163.

[22] Shanghua Gao, Teddy Koker, Owen Queen, Thomas Hartvigsen, Theodoros Tsiligkaridis, and Marinka Zitnik. 2024. UniTS: Building a Unified Time Series Model. *arXiv preprint arXiv:2403.00131* (2024).

[23] Azul Garza, Cristian Challu, and Max Mergenthaler-Canseco. 2023. TimeGPT-1. *arXiv preprint arXiv:2310.03589* (2023).

[24] Ian J Goodfellow, Jonathon Shlens, and Christian Szegedy. 2014. Explaining and harnessing adversarial examples. *arXiv preprint arXiv:1412.6572* (2014).

[25] Mononito Goswami, Konrad Szafer, Arjun Choudhry, Yifu Cai, Shuo Li, and Artur Dubrawski. 2024. MOMENT: A Family of Open Time-series Foundation Models. In *ICML*.

[26] Chuan Guo, Jacob Gardner, Yurong You, Andrew Gordon Wilson, and Kilian Weinberger. 2019. Simple black-box adversarial attacks. In *ICML*. 2484–2493.

[27] Jingxuan He and Martin Vechev. 2023. Large language models for code: Security hardening and adversarial testing. In *SIGSAC*. 1865–1879.

[28] Kai Heinrich, Johannes Graf, Ji Chen, Jakob Laurisch, and Patrick Zschech. 2020. Fool me Once, shame on You, Fool me Twice, shame on me: a Taxonomy of Attack and de-Fense Patterns for AI Security.. In *ECIS*.

[29] Shi Bin Hoo, Samuel Müller, David Salinas, and Frank Hutter. 2025. The tabular foundation model TabPFN outperforms specialized time series forecasting models based on simple features. *arXiv preprint arXiv:2501.02945* (2025).

[30] Andrew Ilyas, Shibani Santurkar, Dimitris Tsipras, Logan Engstrom, Brandon Tran, and Aleksander Madry. 2019. Adversarial examples are not bugs, they are features. In *NeurIPS*.

[31] Fazle Karim, Somshubra Majumdar, and Houshang Darabi. 2020. Adversarial attacks on time series. *IEEE transactions on pattern analysis and machine intelligence* 43, 10 (2020), 3309–3320.

[32] Taesung Kim, Jinhee Kim, Yunwon Tae, Cheonbok Park, Jang-Ho Choi, and Jaegul Choo. 2022. Reversible Instance Normalization for Accurate Time-Series Forecasting against Distribution Shift. In *ICLR*.

[33] Alexander Kirillov, Eric Mintun, Nikhila Ravi, Hanzi Mao, Chloe Rolland, Laura Gustafson, Tete Xiao, Spencer Whitehead, Alexander C Berg, Wan-Yen Lo, et al. 2023. Segment anything. In *ICCV*. 4015–4026.

[34] Alexandros Koulakos, Maria Lymperaiou, Giorgos Filandrianos, and Giorgos Stamou. 2024. Enhancing adversarial robustness in Natural Language Inference using explanations. *arXiv preprint arXiv:2409.07423* (2024).

[35] Yuxuan Liang, Haomin Wen, Yuqi Nie, Yushan Jiang, Ming Jin, Dongjin Song, Shirui Pan, and Qingsong Wen. 2024. Foundation models for time series analysis: A tutorial and survey. In *Proceedings of the 30th ACM SIGKDD conference on knowledge discovery and data mining*. 6555–6565.

[36] Aixin Liu, Bei Feng, Bing Xue, Bingxuan Wang, Bochao Wu, Chengda Lu, Chenggang Zhao, Chengqi Deng, Chenyu Zhang, Chong Ruan, et al. 2024. Deepseek-v3 technical report. *arXiv preprint arXiv:2412.19437* (2024).

[37] Linbo Liu, Youngsuk Park, Trong Nghia Hoang, Hilaf Hasson, and Jun Huan. 2023. Robust multivariate time-series forecasting: Adversarial attacks and defense mechanisms. In *ICLR*.

[38] Ye Liu, Yaya Cheng, Lianli Gao, Xianglong Liu, Qilong Zhang, and Jingkuan Song. 2022. Practical evaluation of adversarial robustness via adaptive auto attack. In *CVPR*. 15105–15114.

[39] Yong Liu, Haoran Zhang, Chenyu Li, Xiangdong Huang, Jianmin Wang, and Mingsheng Long. 2024. Timer: Transformers for Time Series Analysis at Scale. In *ICML*.

[40] Aleksander Madry, Aleksandar Makelov, Ludwig Schmidt, Dimitris Tsipras, and Adrian Vladu. 2017. Towards deep learning models resistant to adversarial attacks. In *ICLR*.

[41] Chengzhi Mao, Amogh Gupta, Vikram Nitin, Baishakhi Ray, Shuran Song, Junfeng Yang, and Carl Vondrick. 2020. Multitask learning strengthens adversarial robustness. In *ECCV*. 158–174.

[42] James E Matheson and Robert L Winkler. 1976. Scoring Rules for Continuous Probability Distributions. *Management Science* 22, 10 (1976), 1087–1096.

[43] Seyed-Mohsen Moosavi-Dezfooli, Alhussein Fawzi, and Pascal Frossard. 2016. Deepfool: a simple and accurate method to fool deep neural networks. In *CVPR*. 2574–2582.

[44] Mohammad Amin Morid, Olivia R Liu Sheng, and Joseph Dunbar. 2023. Time series prediction using deep learning methods in healthcare. *ACM Transactions on Management Information Systems* 14, 1 (2023), 1–29.

[45] Aristeidis Mystakidis, Paraskevas Koukaras, Nikolaos Tsalikidis, Dimosthenis Ioannidis, and Christos Tjortjis. 2024. Energy forecasting: a comprehensive review of techniques and technologies. *Energies* 17, 7 (2024), 1662.

[46] Ethan Perez, Saffron Huang, Francis Song, Trevor Cai, Roman Ring, John Aslanides, Amelia Glaese, Nat McAleese, and Geoffrey Irving. 2022. Red teaming language models with language models. *arXiv preprint arXiv:2202.03286* (2022).

[47] Harshavardhan Prabhakar Kamarthi and B Aditya Prakash. 2024. Large Pre-trained time series models for cross-domain Time series analysis tasks. In *NeurIPS*. 56190–56214.

[48] Joan Puigcerver, Rodolphe Jenatton, Carlos Riquelme, Pranjal Awasthi, and Srinadh Bhojanapalli. 2022. On the adversarial robustness of mixture of experts. In *NeurIPS*. 9660–9671.

[49] Kashif Rasul, Arjun Ashok, Andrew Robert Williams, Hena Ghonia, Rishika Bhagwatkar, Arian Khorasani, Mohammad Javad Darvishi Bayazi, George Adamopoulos, Roland Riachi, Nadhir Hassen, et al. 2023. Lag-Llama: Towards Foundation Models for Probabilistic Time Series Forecasting. *arXiv preprint arXiv:2310.08278* (2023).

[50] Pradeep Rathore, Arghya Basak, Sri Harsha Nistala, and Venkataramana Runkana. 2020. Untargeted, targeted and universal adversarial attacks and defenses on time series. In *IJCNN*. 1–8.

[51] Robin Rombach, Andreas Blattmann, Dominik Lorenz, Patrick Esser, and Björn Ommer. 2022. High-resolution image synthesis with latent diffusion models. In *CVPR*. 10684–10695.

[52] Christian Schlarmann and Matthias Hein. 2023. On the adversarial robustness of multi-modal foundation models. In *ICCV*. 3677–3685.

[53] Erfan Shayegani, Md Abdullah Al Mamun, Yu Fu, Pedram Zaree, Yue Dong, and Nael Abu-Ghazaleh. 2023. Survey of vulnerabilities in large language models revealed by adversarial attacks. *arXiv preprint arXiv:2310.10844* (2023).

[54] Xiaoming Shi, Shiyu Wang, Yuqi Nie, Dianqi Li, Zhou Ye, Qingsong Wen, and Ming Jin. 2025. Time-moe: Billion-scale time series foundation models with mixture of experts. In *ICLR*.

[55] Shoaib Ahmed Siddiqui, Andreas Dengel, and Sheraz Ahmed. 2020. Benchmarking adversarial attacks and defenses for time-series data. In *International Conference on Neural Information Processing*. Springer, 544–554.

[56] Dong Su, Huan Zhang, Hongge Chen, Jinfeng Yi, Pin-Yu Chen, and Yupeng Gao. 2018. Is robustness the cost of accuracy?—a comprehensive study on the robustness of 18 deep image classification models. In *ECCV*. 631–648.

[57] Christian Szegedy, Wojciech Zaremba, Ilya Sutskever, Joan Bruna, Dumitru Erhan, Ian Goodfellow, and Rob Fergus. 2013. Intriguing properties of neural networks. In *ICLR*.

[58] Yajiao Tang, Zhenyu Song, Yulin Zhu, Huaiyu Yuan, Maozhang Hou, Junkai Ji, Cheng Tang, and Jianqiang Li. 2022. A survey on machine learning models for financial time series forecasting. *Neurocomputing* 512 (2022), 363–380.

[59] Hugo Touvron, Louis Martin, Kevin Stone, Peter Albert, Amjad Almahairi, Yasmine Babaei, Nikolay Bashlykov, Soumya Batra, Prajjwal Bhargava, Shruti Bhosale, et al. 2023. Llama 2: Open foundation and fine-tuned chat models. *arXiv preprint arXiv:2307.09288* (2023).

[60] Boxin Wang, Shuohang Wang, Yu Cheng, Zhe Gan, Ruoxi Jia, Bo Li, and Jingjing Liu. 2021. Infobert: Improving robustness of language models from an information theoretic perspective. In *ICLR*.

[61] Xuezhi Wang, Haohan Wang, and Diyi Yang. 2021. Measure and improve robustness in NLP models: A survey. *arXiv preprint arXiv:2112.08313* (2021).

[62] Gerald Woo, Chenghao Liu, Akshat Kumar, Caiming Xiong, Silvio Savarese, and Doyen Sahoo. 2024. Unified Training of Universal Time Series Forecasting Transformers. In *ICML*.

[63] Chin-Chia Michael Yeh, Xin Dai, Huiyuan Chen, Yan Zheng, Yujie Fan, Audrey Der, Vivian Lai, Zhongfang Zhuang, Junpeng Wang, Liang Wang, et al. 2023. Toward a foundation model for time series data. In *CIKM*. 4400–4404.

[64] TaeHo Yoon, Youngsuk Park, Ernest K Ryu, and Yuyang Wang. 2022. Robust probabilistic time series forecasting. In *AISTATS*. 1336–1358.

[65] Hsiang-Fu Yu, Nikhil Rao, and Inderjit S Dhillon. 2016. Temporal regularized matrix factorization for high-dimensional time series prediction. In *NeurIPS*.

[66] Haoran Zhang, Yong Liu, Yunzhong Qiu, Haixuan Liu, Zhongyi Pei, Jianmin Wang, and Mingsheng Long. 2025. Timesbert: A bert-style foundation model for time series understanding. *arXiv preprint arXiv:2502.21245* (2025).

[67] Yunqing Zhao, Tianyu Pang, Chao Du, Xiao Yang, Chongxuan Li, Ngai-Man Man Cheung, and Min Lin. 2023. On evaluating adversarial robustness of large vision-language models. In *NeurIPS*, Vol. 36. 54111–54138.

## A Details of Time Series Foundation Models

Table 3: Comparison of time-series foundation models used in this study.

	TimesFM[13]	TimeMoE[54]	UniTS[22]	Moirai[62]	Chronos[2]	TabPFN[29]
Backbone	Dec-only	Dec-only	Enc-only	Enc-only	Enc-Dec	Enc-only
Decoding	AR	AR	NAR	NAR	AR	NAR
Pos. Emb.	Absolute PE	RoPE	Learnable PE	RoPE	Rel. PE	Calendar
Pred. Head	Point	Point	Point	Dist.	Dist.	Dist.
Loss	MSE	Huber+Aux	MSE	Likelihood	Cross-entropy	Cross-entropy
Patchify	✓	✗	✓	✓	✗	✗
Standardization	ReVIN	ReVIN	ReVIN	ReVIN	Mean scaling	Z-score
Grad-based Att.	✓	✓	✓	✓	✗	✗
Pretrained Model	200M 500M	50M 200M	x32 x128	small (13.8M) base (91.4M) large (311M)	tiny (8M) mini (20M) small (46M) base (200M) large (710M)	11M

**Backbone and Decoding Strategy.** TimesFM, Chronos and TimeMoE adopt decoder-only Transformer architectures with autoregressive (AR) decoding, closely following the design of large language models. UniTS, TabPFN-TS and Moirai use encoder-only backbones with non-autoregressive (NAR) decoding, enabling parallel prediction across time steps.

**Prediction Head and Loss.** TimesFM, TimeMoE, and UniTS perform point forecasting optimized with MSE or Huber losses. In contrast, Moirai, Chronos, and TabPFN-TS adopt distributional forecasting heads trained with likelihood-based or cross-entropy losses.

**Input Patchification and Normalization.** Most encoder-based models adopt input patchification to improve modeling efficiency, except Chronos and TabPFN. For standardization, all models except Chronos and TabPFN use ReVIN [32], a reversible instance normalization technique tailored for time series. Chronos applies mean scaling, while TabPFN uses z-score normalization.

**Gradient-based Attack Compatibility.** Not all models are compatible with gradient-based white-box attacks. TimesFM, TimeMoE, UniTS, and Moirai produce continuous outputs, allowing direct optimization through gradient-based methods such as PGD. In contrast, Chronos and TabPFN-TS discretize both inputs and outputs by treating time points as tokens and generating categorical distributions over predefined bins. This discretization renders standard gradient-based attacks impractical.

## B Details of Evaluation Protocols

Algorithm 1 summarizes the core procedure, where the attacker perturbs the input sequence  $\mathbf{x}_{t-L:t}$  within a constrained budget to either increase forecast error (untargeted) or drive the output toward a predefined target trajectory (targeted).

### B.1 Attacking Strategies

**Projected Gradient Descent (PGD)** PGD [40] is a white-box attack that iteratively perturbs the input in the direction of the gradient of the loss with respect to the input. At each step, the perturbation is projected back onto the feasible  $\ell_p$ -norm ball to ensure it stays within the allowed budget. The update rule is given by:

$$\mathbf{x}^{k+1} = \Pi_{\mathcal{B}_p(\mathbf{x}, \epsilon)} (\mathbf{x}^k + \alpha \cdot \text{sign} (\nabla_{\mathbf{x}} \mathcal{L}(f_{\phi}(\mathbf{x}^k), y))), \quad (9)$$

where  $\Pi$  denotes the projection operator,  $\mathcal{L}$  is the loss function,  $f_{\phi}$  is the model,  $\epsilon$  is the perturbation budget, and  $\alpha$  is the step size.

---

**Algorithm 1** TSFM Adversarial Robustness Evaluation

---

**Require:** Pre-trained model  $f_\phi$ , input  $\mathbf{x}_{t-L:t}$ , budget  $(r, \epsilon)$ , attack type  $\sigma \in \{+1, -1\}$ , transform params  $(a, c(\cdot))$

- 1:  $\hat{\mathbf{x}}^{\text{clean}} \leftarrow f_\phi(\mathbf{x}_{t-L:t})$  ▷ Sec. 3.1
- 2: **if**  $\sigma = +1$  **then** ▷ untargeted
- 3:      $\mathbf{y} \leftarrow \hat{\mathbf{x}}^{\text{clean}}$
- 4: **else** ▷ targeted
- 5:      $\mathbf{y} \leftarrow \mathcal{M}(\hat{\mathbf{x}}^{\text{clean}}; a, c)$  ▷ Eq. (3)
- 6: **end if**
- 7:  $\mathcal{S} \leftarrow \{\delta : \|\delta\|_0 \leq rL, \|\delta\|_\infty \leq \epsilon\}$  ▷ Eq. (4)
- 8:  $\delta^* \leftarrow \text{ATTACK}(f_\phi, \mathbf{x}_{t-L:t}, \mathbf{y}, \mathcal{S}, \sigma)$  ▷ Sec. 3.3
- 9:  $\hat{\mathbf{x}}^{\text{adv}} \leftarrow f_\phi(\mathbf{x}_{t-L:t} + \delta^*)$
- 10:  $\text{RED}_\mathcal{E} \leftarrow \text{COMPUTERED}(\hat{\mathbf{x}}^{\text{clean}}, \hat{\mathbf{x}}^{\text{adv}}, \mathbf{y})$  ▷ Eq. (8)
- 11: **return**  $\hat{\mathbf{x}}^{\text{adv}}, \text{RED}_\mathcal{E}$

---

**Zeroth Order Optimization (ZOO)** ZOO [8] is a black-box attack that approximates the gradient using only function evaluations, without requiring access to the model’s internals. The directional derivative is estimated using finite differences:

$$\frac{\partial \mathcal{L}}{\partial x_i} \approx \frac{\mathcal{L}(\mathbf{x} + h\mathbf{e}_i) - \mathcal{L}(\mathbf{x} - h\mathbf{e}_i)}{2h}, \quad (10)$$

where  $h$  is a small constant, and  $\mathbf{e}_i$  is the standard basis vector in the  $i$ -th direction. The estimated gradients are then used to perform gradient-based optimization in the black-box setting.

**Simple Black-box Attack (SimBA).** SimBA [26] is a decision-based black-box attack that perturbs the input along randomly selected directions from an orthonormal basis. At each iteration, a candidate direction  $\mathbf{q} \in Q$  and step size  $\epsilon > 0$  are selected. The algorithm tries  $\mathbf{x} + \epsilon\mathbf{q}$ ; if the model’s predicted probability  $p_h(y | \mathbf{x})$  decreases, the step is accepted. Otherwise, it tries  $\mathbf{x} - \epsilon\mathbf{q}$  and accepts it if it reduces  $p_h(y | \mathbf{x})$ . To ensure efficiency, SimBA samples directions without replacement and guarantees a bounded  $\ell_2$ -norm of the perturbation:  $\|\delta\|_2 = \sqrt{T}\epsilon$  after  $T$  updates. Its only hyperparameters are the set of orthonormal vectors  $Q$  and the step size  $\epsilon$ .

1. **Cartesian Basis (Point-wise):** The *standard basis*  $Q_{\text{ID}} = \{\mathbf{e}_1, \dots, \mathbf{e}_L\}$  consists of unit vectors, where each  $\mathbf{e}_i \in \mathbb{R}^L$  has a 1 at the  $i$ -th position and zeros elsewhere. This basis corresponds to perturbing individual time points independently. Each attack iteration modifies a single, randomly selected time step by increasing or decreasing its value.
2. **Discrete Cosine Transform (DCT) Basis:** The *DCT basis*  $Q_{\text{DCT}}$  is an orthonormal set of vectors that transform a time-domain signal  $x \in \mathbb{R}^L$  into a sequence of frequency coefficients. To encourage smooth and perceptually coherent perturbations, we restrict the perturbation to lie within a low-frequency subspace. Specifically, we retain only a fraction  $r \in (0, 1]$  of the lowest-frequency components from  $Q_{\text{DCT}}$ .
3. **Wavelet Basis:** The *wavelet basis*  $Q_{\text{WAV}}$  is derived from a discrete wavelet transform (DWT), such as the Haar family. This basis provides a time-frequency decomposition, where each vector captures information localized in both time and scale (resolution). Perturbations in this basis can target specific trends or local details. For control over the granularity of perturbation, we optionally restrict  $Q_{\text{WAV}}$  to low-frequency (approximation) coefficients at a specified decomposition level  $\ell$ .

## B.2 Metrics

**The Normalized Mean Absolute Error (NMAE)** The Normalized Mean Absolute Error (NMAE) [65] is a normalized version of the MAE, which is dimensionless and facilitates the comparability of the error magnitude across different datasets or scales. The mathematical representation of NMAE is given by:

$$\text{NMAE} = \frac{\sum_{t=1}^T |x_t - \hat{x}_t|}{\sum_{t=1}^T |x_t|}.$$

**Normalized Root Mean Squared Error (NRMSE)** The Normalized Root Mean Squared Error (NRMSE) is a normalized version of the Root Mean Squared Error (RMSE), which quantifies the average squared magnitude of the error between forecasts and observations, normalized by the expectation of the observed values. It can be formally written as:

$$\text{NRMSE} = \frac{\sqrt{\frac{1}{T} \sum_{t=1}^T (x_t - \hat{x}_t)^2}}{\frac{1}{T} \sum_{t=1}^T |x_t|}.$$

**Continuous Ranked Probability Score (CRPS)** The Continuous Ranked Probability Score (CRPS) [42] quantifies the agreement between a cumulative distribution function (CDF)  $F$  and an observation  $x$ , represented as:

$$\text{CRPS} = \int_{\mathbb{R}} (F(z) - \mathbb{I}\{x \leq z\})^2 dz,$$

where  $\mathbb{I}\{x \leq z\}$  denotes the indicator function, equating to one if  $x \leq z$  and zero otherwise.

Being a proper scoring function, CRPS reaches its minimum when the predictive distribution  $F$  coincides with the data distribution. When using the empirical CDF of  $F$ , denoted as  $\hat{F}(z) = \frac{1}{n} \sum_{i=1}^n \mathbb{I}\{X_i \leq z\}$ , where  $n$  represents the number of samples  $X_i \sim F$ , CRPS can be precisely calculated from the simulated samples of the conditional distribution  $p_{\theta}(\mathbf{x}_t | \mathbf{h}_t)$ . In our practice, 100 samples are employed to estimate the empirical CDF.

## C Additional Details of Experiment Setting

### C.1 Dataset Details

We adopt benchmark datasets from the GIFT-Eval benchmark [1], which includes a diverse set of real-world time-series datasets covering multiple domains, sampling granularities, and forecasting settings. For this study, we select a subset of these datasets to ensure broad domain coverage. A complete summary of the dataset characteristics, including domain, number of target variables, number of series, sampling frequency, input windows, and prediction lengths, is provided in Table 4.

Table 4: Summary of datasets used in our experiments. Datasets such as Solar, Electricity, and ETT support short-, medium-, and long-term forecasting settings, while others like US Births and Hierarchical Sales are limited to short-term prediction scenarios.

Dataset	Domain	#Target Var	# Series	Frequency	# Windows	Pred Len
Solar	Energy	1	137	10T H	20/11/8 29/2/2	48/480/720
Electricity	Energy	1	370	15T H	20/20/20 20/8/5	48/480/720
ETT1	Energy	7	1	15T H	20/15/10 20/4/3	48/480/720
Loop Seattle	Transport	1	323	5T H	20/20/15 19/2/2	48/480/720
BizTObs - L2C	Web/CloudOps	7	1	5T H	20/7/5 6/1/1	48/480/720
Jena Weather	Nature	21	1	10T H	20/11/8 19/2/2	48/480/720
US Births	Healthcare	1	1	D/W/M	20/14/2	30/8/12
Hierarchical Sales	Sales	1	118	D/W	7/4	30/8

## D Additional Experimental Results

### D.1 Performance Comparison of TSFMs

In Table 5, we present the forecasting performance of six TSFMs on unperturbed inputs across eight datasets. Among all models, TimesFM consistently achieves strong zero-shot forecasting performance across diverse domains, followed closely by Moirai. This highlights the benefit of large-scale pretraining and architectural generality. However, our robustness evaluation reveals that stronger predictive accuracy does not necessarily imply higher adversarial resilience. In fact, these high-performing models often exhibit greater vulnerability to adversarial perturbations. This observation underscores a critical challenge: how to effectively balance predictive accuracy and robustness in the design of TSFMs. Addressing this trade-off remains an open and urgent research direction.

Table 5: **Raw forecasting performance of TSFMs across multiple datasets.** All results are reported under the short-term setting with context length 128. We evaluate each model using three metrics: NMAE, NRMSE, and CRPS. The best result for each metric is **bolded**, and the second best is underlined.

Dataset	NMAE	Chronos	CRPS	NMAE	Moirai	CRPS	NMAE	TimeMoE	CRPS	NMAE	TimesFM	UniTS	NRMSE	CRPS
Loop Seattle	0.08	0.10	0.13	0.07	<b>0.07</b>	<b>0.10</b>	0.10	0.10	0.13	<b>0.06</b>	0.08	0.11	0.07	0.08
BizITObs-L2C	1.16	1.42	1.86	1.19	<u>1.19</u>	<b>1.54</b>	1.43	1.77	1.22	1.46	1.99	<b>0.91</b>	<b>1.00</b>	1.55
Electricity	0.28	0.33	0.45	0.27	<b>0.27</b>	<b>0.38</b>	0.34	0.34	0.45	0.28	0.34	0.45	0.27	0.32
ETT1	0.23	0.27	0.52	0.27	0.27	0.48	0.33	0.33	0.56	<u>0.22</u>	0.27	0.50	0.23	0.27
Hierarchical Sales	<b>0.75</b>	<b>0.89</b>	<b>1.66</b>	1.29	1.29	1.89	1.44	1.44	2.13	0.87	1.00	1.78	0.80	0.95
Jena Weather	0.05	0.06	0.22	0.21	0.21	0.34	0.08	0.08	0.26	0.06	0.07	0.28	0.05	0.06
Solar	0.50	0.59	0.96	0.41	0.41	<b>0.71</b>	0.92	0.92	1.19	0.41	0.52	0.97	<b>0.36</b>	<b>0.40</b>
US Births	0.03	0.03	0.04	0.03	0.03	0.04	0.10	0.10	0.12	0.04	0.05	0.06	<b>0.02</b>	<b>0.03</b>
													<b>0.04</b>	<b>0.04</b>

### D.2 Additional Metrics for Evaluation

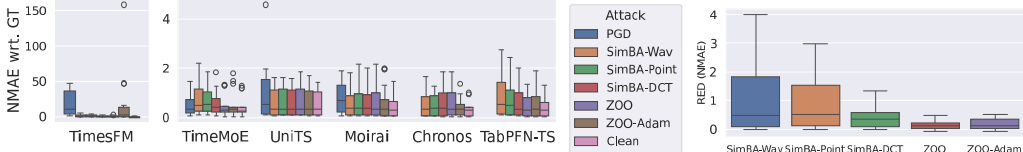
As a supplement to Table 2, we report the  $\text{RED}_{\text{CRPS}}$  scores under untargeted attacks in Table 6. CRPS is a widely used metric for evaluating the quality of probabilistic forecasts. We observe that the robustness rankings across models based on CRPS are largely consistent with those based on NMAE.

Table 6: **Untargeted attacks against TSFMs.** We report the  $\text{RED}_{\text{CRPS}}$  averaged across attack budgets ( $\epsilon \in \{0.25, 0.5, 0.75, 1\}$ ,  $r \in \{0.25, 0.5, 0.75, 1\}$ ) and datasets. **Red** is used to denote the model most impacted by the attack.

Dataset	PGD				SimBA (Wavelet)					
	TimesFM	TimeMoE	UniTS	Moirai	TimesFM	TimeMoE	UniTS	Moirai	Chronos	TabPFN-TS
Loop Seattle	27.35	0.25	0.34	1.74	0.93	0.39	0.01	0.41	0.13	0.82
BizITObs-L2C	15.39	0.22	0.43	0.41	1.65	0.47	0.13	0.35	0.15	0.53
Electricity	27.45	0.19	0.18	0.35	1.42	0.37	0.00	0.05	0.03	0.48
ETT1	32.80	0.20	0.58	1.69	1.68	0.80	0.06	0.59	0.54	1.37
Hierarchical Sales	44.72	0.08	1.46	1.04	3.87	0.71	0.23	0.35	0.51	2.09
Jena Weather	37.87	0.04	0.40	0.63	2.12	0.41	0.04	0.10	0.24	1.11
Solar	48.11	0.65	0.34	1.09	3.03	1.43	0.06	0.78	0.59	1.47
US Births	30.59	0.81	0.06	0.70	3.35	1.60	-0.01	0.41	1.06	2.47

### D.3 Effectiveness of Attack Strategies

Figure 7a compares the effectiveness of different attack strategies across various TSFMs under a fixed perturbation budget (untargeted attacks,  $\epsilon = 0.5$ ,  $r = 1$ ). We observe that all TSFMs are vulnerable to adversarial perturbations, with varying degrees of susceptibility. Among the attack methods, PGD consistently achieves the strongest performance, followed by SimBA and then ZOO. For SimBA variants, the choice of perturbation basis significantly impacts effectiveness: wavelet-based directions perform best, followed by point-wise and DCT bases. These results highlight both the vulnerability of current TSFMs and the importance of attack design choices, including basis structure and optimization method, in determining attack success.



(a) Attack performance across TSFMs. TimesFM is shown separately due to its large performance variance under PGD.  
(b) Comparison of black-box attacks.

Figure 7: **Effectiveness of untargeted adversarial attacks across different strategies.** We evaluate PGD, SimBA (with wavelet, point, and DCT bases), and ZOO (with standard and Adam optimizers) under a fixed budget of  $\epsilon = 0.5$ ,  $r = 1$ . Results are averaged over all datasets.

#### D.4 Model Robustness Under Varying Perturbation Budgets

Figure 8 presents robustness curves for each dataset under SimBA attacks, where we vary the perturbation budget  $\epsilon$  and fix the attack ratio  $r = 1$ . These plots reveal that model robustness is highly dataset-dependent. For example, Moirai remains stable on US Births but degrades significantly on BizTObs-L2C, while TimesFM exhibits sharp performance drops across most datasets, indicating high vulnerability. In contrast, models like UniTS and Chronos show relatively moderate and consistent degradation. These results highlight the challenge of building TSFMs that are both accurate and robust across diverse real-world scenarios. Achieving such consistency remains a key open problem for safe and reliable deployment.

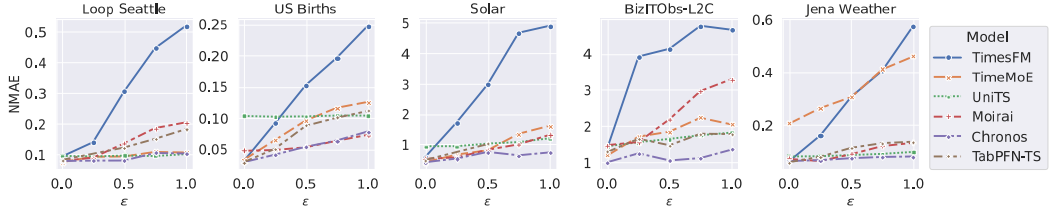


Figure 8: **Model robustness under SimBA attack across datasets.** We report the degradation in NMAE as the perturbation bound  $\epsilon$  increases, with attack ratio  $r = 1$ .

#### D.5 Full Results of Targeted Attacks

Table 7 and Table 8 report  $\text{RED}_{\text{NMAE}}$  scores under targeted attacks. We find that **global-targeted attacks** (e.g., scaling or shifting the full forecast) are generally more effective than **local-targeted attacks** (e.g., modifying a subsegment). This suggests that TSFMs often lack strong global constraints, making them susceptible to trajectory-wide manipulations. In contrast, localized targets are harder to exploit, likely due to inductive biases that enforce smoothness and temporal consistency—making it difficult to alter specific time steps without disrupting the overall sequence.

Table 7: **Targeted attacks (scaling and drifting) on TSFMs.** We report the averaged  $\text{RED}_{\text{NMAE}}$  across different attack budgets ( $\epsilon \in \{0.25, 0.5, 0.75, 1\}$ ,  $r \in \{0.25, 0.5, 0.75, 1\}$ ) on various datasets. **Red** highlights denote successful attacks where the perturbed forecasts move closer to the target. **Green** denote unsuccessful attacks where predictions deviate further from the target.

Model	PGD					SimBA				
	$a = -1.0$	$a = 0.5$	$a = 2$	$\beta = 0.05$	$\beta = 0.1$	$a = -1.0$	$a = 0.5$	$a = 2$	$\beta = 0.05$	$\beta = 0.1$
TimesFM	0.578	0.697	0.618	0.775	0.796	0.418	0.607	0.510	0.634	0.590
TimeMoE	0.225	-0.131	-0.021	0.145	0.124	0.416	0.599	0.379	0.538	0.460
UniTS	0.447	-0.757	-0.007	-0.172	0.091	0.137	-0.397	-0.398	-0.100	0.035
Moirai	0.475	0.595	0.323	0.604	0.637	0.178	0.159	0.021	0.294	0.251
Chronos	-	-	-	-	-	0.055	-0.138	-0.157	0.023	0.059
TabPFN-TS	-	-	-	-	-	0.365	0.688	0.476	0.484	0.486

Table 8: **Targeted attacks (local offset) on TSFMs.** We report the Average Relative Error Deviation across different attack budgets ( $\epsilon \in \{0.25, 0.5, 0.75, 1\}$ ,  $r \in \{0.25, 0.5, 0.75, 1\}$ ) on various datasets. We denote the perturbed region in the prediction horizon as  $\langle \tau_{\text{start}}, \tau_{\text{end}} \rangle$ , where  $\tau \in [0, 1]$  is a normalized index ( $\tau = 0$  corresponds to the first time step, and  $\tau = 1$  to the last).

Model	PGD				SimBA			
	$\langle 0.75, 1 \rangle$	$\langle 0, 0.25 \rangle$	$\langle 0.5, 1 \rangle$	$\langle 0, 0.5 \rangle$	$\langle 0.75, 1 \rangle$	$\langle 0, 0.25 \rangle$	$\langle 0.5, 1 \rangle$	$\langle 0, 0.5 \rangle$
TimesFM	0.294	0.265	0.465	0.433	-0.100	-0.099	0.193	0.194
TimeMoE	<b>-3.755</b>	<b>-3.847</b>	<b>-1.537</b>	<b>-1.699</b>	-0.899	-0.942	-0.193	-0.041
UniTS	<b>-6.162</b>	<b>-5.984</b>	<b>-2.610</b>	<b>-2.511</b>	<b>-5.066</b>	<b>-4.611</b>	<b>-2.260</b>	<b>-2.044</b>
Moirai	0.013	0.052	0.117	0.186	-0.364	-0.321	-0.252	-0.163
Chronos	-	-	-	-	-0.611	-0.648	-0.492	-0.403
TabPFN-TS	-	-	-	-	-1.068	-1.062	-0.152	-0.352

## D.6 Model performance under Different Model Size

In Table 9, we compare the vulnerability of TSFMs with different parameter scales under both white-box (PGD) and black-box (SimBA) attacks. We observe that under white-box attacks, larger models tend to suffer greater performance degradation, consistent with prior findings [30]. An exception is TimesFM-500M, whose better robustness is likely attributable to its weak raw performance rather than model size. Under black-box attacks, however, there is no clear correlation between model size and vulnerability.

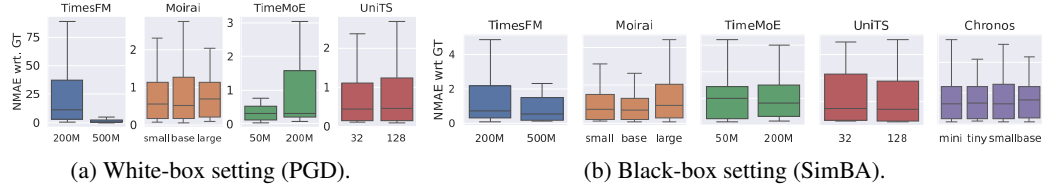


Figure 9: **Impact of model size on robustness under different attack strategies.** We evaluate TSFMs of varying scales under PGD and SimBA attacks, with fixed budget  $\epsilon = 0.5$ ,  $r = 1$ .

## D.7 Robustness under Different Prediction Horizons

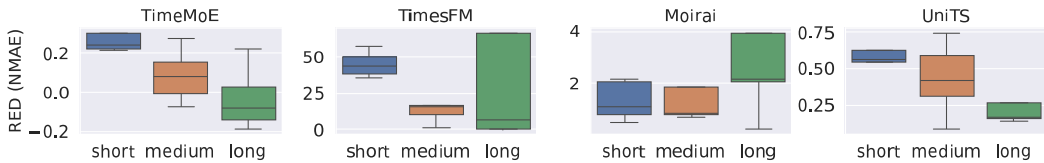


Figure 10: **Robustness under different prediction horizons.** RED<sub>NMAE</sub> of four TSFMs under PGD attacks with  $\epsilon = 0.5$  and attack ratio  $r = 1$ . For short-term forecasting, the context length is set to 128; for medium- and long-term settings, it is 256.

Figure 10 compares the robustness scores (RED<sub>NMAE</sub>) of four TSFMs under PGD attacks across different prediction horizons. We observe that, in most cases, short-term forecasting is more susceptible to adversarial perturbations. One possible explanation is that long-term forecasts are inherently less accurate, leading to lower baseline performance and therefore smaller relative error degradation (RED). An exception is Moirai, which exhibits a substantial drop in performance under adversarial attacks in the long-term setting, indicating heightened vulnerability in this regime.